mitte etwas bei. Man wird also erwarten, daß die Flügel der aus Achsennähe emittierten Linien durch die Randzonen unbeeinflußt bleiben.

Wendet man an Stelle der Halbwertsbreite eine Vergleichsgröße an, die mehr im Linienflügel liegt – z. B. den Wellenlängenabstand $(Z-H)$ zwischen den beiden Punkten, zwischen welchen die Intensität von 1/2 auf 1/10 der Maximalintensität abgenommen hat –, so kann man erwarten, daß die Elektronendichte unter der gemachten Voraussetzung auch ohne ABEL-Inversion in guter Näherung gefunden werden kann.

Die in Abb. 3 dargestellten Elektronendichteprofile wurden auf die beschriebene Weise mit Hilfe der Vergleichsgröße $(Z-H)$ ermittelt. Die Genauigkeit des Verfahrens wurde für den Bogen (a) überprüft. Dazu wurde das gemessene Temperatur- und Elektronendichteprofil des Bogens durch je ein Treppenprofil mit fünf Stufen ersetzt. Für jede Stufe wurde nach [7] die Kontur der H_γ-Linie berechnet. Aus der Überlagerung der Strahlung der verschiedenen Zonen erhält man die entsprechenden „side-on"-Profile der Linie. Ein Vergleich mit den Ausgangsprofilen zeigte, daß die unter Verwendung von $(Z-H)$ bestimmte Elektronendichte in der Bogenmitte um etwa 20% zu klein ist. (Der aus der Halbwertsbreite erhaltene Wert dagegen hätte einen Fehler von 40%.) Dies wirkt sich bei der Temperaturbestimmung nach Verfahren b) so aus, daß die Temperaturwerte in der Bogenachse zu klein ausfallen; am Rande dagegen ist die Methode genau.

Spallation, Fission, and Neutron Capture Anomalies in Meteoritic Krypton and Xenon

K. MARTI *, P. EBERHARDT, and J. GEISS

Physikalisches Institut, University of Berne, Switzerland

(Z. Naturforschg. **21 a**, 398—413 [1966]; received 19 November 1965)

Measurements of the Kr and Xe concentrations and isotopic compositions in five meteorites are reported. Experimental techniques and reproducibility are discussed in detail. In the Stannern achondrite 75% of the total Kr and 30% of the total Xe are due to cosmic ray induced spallation reactions. Also Bruderheim and H-Ausson show distinct spallation components. The isotopic composition of pure spallation Kr is derived as

$$Kr^{78} : Kr^{80} : Kr^{82} : Kr^{83} : Kr^{84} = 0.179 : 0.495 : 0.765 : 1.00 : 0.63$$

and of spallation Xe as

$$Xe^{124} : Xe^{126} : Xe^{128} : Xe^{130} : Xe^{131} : Xe^{132} = 0.590 : 1.00 : 1.45 : 0.97 : 3.9 : 0.9\,.$$

It is shown that the spallation components found were produced by the cosmic radiation late in the history of the meteorite during a period given by the radiation age. The observed Xe^{126}/Xe^{124} spallation ratio rules out a substantial contribution of spallation products in the xenon of carbonaceous chondrites. The Xe fission spectrum derived by ROWE and KURODA from Pasamonte is corrected for spallation and the following composition is obtained for fission Xe:

$$Xe^{131} : Xe^{132} : Xe^{134} : Xe^{136} = 0.22 : 1.00 : 1.02 : 1.00\,.$$

In Mezö-Madaras and Abee Kr^{80}, Kr^{82} and Xe^{128} excesses are found, due to (n,γ) reactions on Br and I. It is shown that neutrons produced by the cosmic radiation during the radiation age can account for the observed effect in Abee and the evidence so far suggests that this is also true for Mezö-Madaras.

1. Introduction

The concentrations and isotopic composition of xenon in meteorites have been investigated with considerable detail by REYNOLDS and his coworkers [1–5] and others [6, 7]. Meteoritic xenon is a mixture of components which can originate from many different sources, such as the decay of I^{129}, fission of uranium and possibly of transuranium elements, cosmic ray induced spallation reactions and (n,γ)

* Present address: Department of Chemistry, University of California, La Jolla, Calif., U.S.A.

[1] J. H. REYNOLDS, Phys. Rev. Letters **4**, 351 [1960].
[2] D. KRUMMENACHER, C. M. MERRIHUE, R. O. PEPIN, and J. H. REYNOLDS, Geochim. Cosmochim. Acta **26**, 231 [1962].
[3] J. H. REYNOLDS, J. Geophys. Res. **68**, 2939 [1963].
[4] C. M. MERRIHUE, J. Geophys. Res. **68**, 325 [1963].
[5] R. O. PEPIN, in The Origin and Evolution of Atmospheres and Oceans (P. J. BRANCAZIO and A. G. W. CAMERON ed.), J. Wiley and Sons, New York 1964, p. 191.
[6] W. B. CLARKE and H. G. THODE, in Isotopic and Cosmic Chemistry, dedicated to H. C. UREY (H. CRAIG, S. L. MILLER, and G. J. WASSERBURG ed.), North Holland Publ. Co., Amsterdam 1964, p. 471.
[7] M. W. ROWE and P. K. KURODA, J. Geophys. Res. **70**, 709 [1965].

reactions. In addition, varying amounts of trapped xenon (primordial xenon) have been found in all investigated meteorites. Sophisticated experimental techniques have to be applied to disentangle these different components [3]. Results of xenon measurements allow important conclusions to be drawn, concerning the history and conditions prevailing during the formation of meteorites and the solar system. Some of these conclusions, such as the proposed particle irradiation during the early history of the solar system, are, however, based on rather marginal evidence.

The isotopic composition of meteoritic krypton has been investigated less extensively. Anomalies due to spallation reactions and neutron capture in bromine and selenium were reported by CLARKE and THODE [8].

In this paper we report and discuss krypton and xenon measurements on five stone meteorites. One of our main objectives was to investigate the spallation components of meteoritic krypton and xenon and to measure their production rates. In order to enhance the spallation component as opposed to the contribution from other sources, we have selected two meteorites with high but different radiation ages and low trapped gas contents (H-Ausson, Bruderheim) and one meteorite with high Sr, Ba and rare earth concentrations (Stannern). If the spallation component in these meteorites was produced by the cosmic radiation late in the history of the meteorite, it should be proportional to the radiation age and to the concentrations of the target elements (Sr, Zr, Ba, and rare earth elements). For comparison, two meteorites with high trapped gas content (Abee and Mezö-Madaras) were chosen.

2. Meteorite Samples

The sources of our meteorite samples are listed in Table 1, along with other relevant data. The chondrite specimen designated as H-Ausson was sold to us as belonging to the observed fall Ausson. However, we have shown that our specimen is probably mislabeled [13] and have consequently designated it as H-Ausson.

Aliquots of the crushed samples from our helium, neon and argon determinations [13] were available for Bruderheim, H-Ausson and Mezö-Madaras. Stannern was prepared according to the technique described elsewhere [13]. The Abee sample which we received was already powdered. Samples between 100mg and 2.5 g were used, depending on the rare gas content.

3. Experimental Technique

3.1 Rare Gas Extraction and Concentration Determinations

Two different rare gas extraction systems were used: System I was connected directly to the mass spectrometer. The sample was melted in an alundum crucible with a molybdenum insert. The crucible was heated by an internal tungsten heater. Two radiation shields were used. The metal vacuum jacket was water cooled. The meteorite samples, wrapped in Al-foil, were stored in a glass side tube and could be dropped through a fun-

meteorite	sample number	date of fall	recovered weight kg	classification	K-Ar age m.y.	radiation age m.y.	source of sample
Abee*	BE-263	6.10.1952	107	enstatite chondrite	4700	6	b
Bruderheim	BE-70	3.4.1960	300	hypersthene chondrite	1900	26	c
H-Ausson	BE-53	unknown	—	bronzite chondrite	4400	50	d
Mezö-Madaras	BE-175	9.4.1852	23	hypersthene chondrite	2000	26	a
Stannern	BE-234	5.22.1808	52	eucrite	3700	~30**	a

Table 1. Some relevant data on the investigated meteorites. Data from PRIOR and HEY [9]; KEIL [10]; STAUFFER [11]; KIRSTEN, KRANKOWSKY, and ZÄHRINGER [12]; EBERHARDT, EUGSTER, GEISS, and MARTI [13]. — Sources of samples: [a] Prof. W. SCHOLLER, Naturhistorisches Museum, Wien; [b] Dr. F. BEGEMANN, Max-Planck-Institut, Mainz; [c] Prof. R. E. FOLINSBEE, University of Alberta Edmonton; [d] Deyrolle, Paris. * Sample from center of meteorite. ** The radiation age of Stannern was estimated from the Ar^{38} and Ne^{21} concentrations because some He^3 diffusion loss may have occurred in this meteorite [11].

[8] W. B. CLARKE and H. G. THODE, J. Geophys. Res. **69**, 3673 [1964].
[9] G. T. PRIOR and M. H. HEY, Catalogue of Meteorites, British Museum, London 1953.
[10] K. KEIL, Fortschr. Mineral. **38**, 202 [1960].
[11] H. STAUFFER, J. Geophys. Res. **67**, 2023 [1962].
[12] T. KIRSTEN, D. KRANKOWSKY, and J. ZÄHRINGER, Geochim. Cosmochim. Acta **27**, 13 [1963].
[13] P. EBERHARDT, O. EUGSTER, J. GEISS, and K. MARTI, Z. Naturforschg. **21 a**, 414 [1966].

nel into the crucible. The extracted gases were cleaned with a Ti-Zr-sponge getter, a hot CuO – Pd mixture, hot Ti-foil and a hot tungsten ribbon. System II is our standard rare gas extraction system used for the determination of the light rare gases as described by EBERHARDT, EUGSTER, GEISS, and MARTI [13].

Both systems were free of mercury and had no cold traps. Prior to the extraction they were thoroughly baked at 300 °C and the extraction crucible degassed. The samples were heated to 70 °C in order to release adsorbed atmospheric gases. During the extraction the entire systems were kept at approximately 70 °C to avoid adsorption of krypton and xenon. Re-extractions at an increased crucible temperature showed that for both systems the extraction yield was better than 98%.

Prior to the mass spectrometric analyses Xe, Kr, and Ar were separated from He and Ne and from each other by adsorption on charcoal. This was necessary to avoid excessive memory due to high ion currents in the mass spectrometer and to exclude interference on mass 80 from Ar^{40}. Xenon was adsorbed at −78 °C (dry ice-ethanol mixture), Kr at −120 °C (melting point of dry ice-ethanol mixture) and Ar at liquid air temperature. The xenon fraction always contained more than 60% of the Xe; the krypton fraction contained approximately 50% of the Kr and $\lesssim$ 1% of the Ar. No isotopic fractionations due to the separation procedure were detected.

Extraction blanks of both systems were frequently determined from extractions on empty Al-containers and from re-extractions. The blank of system I was 15×10^{-12} cc STP Kr and 3×10^{-12} cc STP Xe; of system II 4×10^{-12} cc STP Kr and 2×10^{-12} cc STP Xe. Extraction system II was also superior in regard to residual organic impurities and had a much lower failure rate. Thus, for most results reported in this paper extraction system II was used.

At least two aliquots of the same sample were extracted to determine the isotopic composition and the reproducibility for each meteorite. The sample size was varied by at least a factor of 2 between these two determinations. Table 2 gives a comparison of the krypton and xenon isotopic compositions obtained in the two analyses of the Stannern achondrite. The agreement is very good, in spite of the low rare gas concentrations and the large anomalies. Also the duplicate analyses of the other meteorites always agreed within the errors given in Tables 4 and 5.

The absolute concentration of xenon was determined in additional extractions using the isotopic dilution method. In order to avoid memory effects, no Xe^{128} spike from irradiated iodine was used. For Abee, which has a large Xe^{129} anomaly, atmospheric xenon was added as spike. The xenon of Abee was used as spike for the other four meteorites by adding small, known amounts of Abee to the meteorite sample. Table 3 gives the results of duplicated isotopic dilution determinations of xenon.

meteorite	sample weight mg	spike	$Xe^{132} \times 10^{-12}$ ccSTP/gm
Abee	150	air xenon standard I	618
Abee	360	air xenon standard II	608
Mezö-Madaras	130	Abee (86 mg)	2050
Mezö-Madaras*	100	air xenon standard I	2200*
Stannern	500	Abee (30 mg)	25.1
Stannern	730	Abee (40 mg)	25.0

Table 3. Reproducibility of xenon concentration measurements with isotopic dilution. * This determination has an error of 10% because the Xe^{129} anomaly in Mezö-Madaras is only 25%.

The krypton concentrations were determined from Kr ion beam intensities in the argon, krypton and xenon fractions. Furthermore, the Kr/Xe ratio (corrected for the different mass spectrometer sensitivity for Kr and Xe) was measured in the unseparated Ar-Kr-Xe fraction of an additional extraction. Kr concentrations were then calculated from the known Xe concentrations. In addition an isotopic dilution determination for Stannern was carried out with Abee as spike. These different modes of the determination of the Kr concentrations always agreed within the limits of error given in Table 4.

sample weight gm	Kr^{78}	Kr^{80}	Kr^{82}	Kr^{83}	Kr^{84}	Kr^{86}			
2.45	70.0	199	341	431	482	100			
0.78	70.5	200	340	427	485	100			
sample weight gm	Xe^{124}	Xe^{126}	Xe^{128}	Xe^{129}	Xe^{130}	Xe^{131}	Xe^{132}	Xe^{134}	Xe^{136}
2.45	7.6	12.7	23.8	98.8	23.0	108.9	100	45.0	40.4
0.78	7.6	12.7	23.6	95.6	23.1	108.5	100	45.1	40.5

Table 2. Comparison of the krypton and xenon isotopic compositions of the two analyses of the Stannern achondrite.

3.2 Mass Spectrometry

The rare gas samples were analyzed in a new, all-glass, sector type, 60 degree, 10 cm radius of curvature, UHV mass spectrometer. The ion current could be measured either with a FARADAY collector or with an electron multiplier. Switchover from one collector to the other could be made in a few seconds. With a source magnet and a total electron emission of 1 mA, the sensitivity of the spectrometer is 0.6×10^{-4} ions/atom sec for krypton and 0.8×10^{-4} ions/atom sec for xenon. This sensitivity corresponds to a detection limit of 2×10^{-15} cc STP per isotope. The mass discrimination was determined by measuring atmospheric krypton and xenon. NIER's [14] values for their isotopic composition were used. All results are corrected for mass discrimination, which was always less than 0.4% per mass unit.

The total amounts of krypton and xenon admitted to the mass spectrometer, including standards, were always kept below a few 10^{-9} cc STP and the instrument was baked frequently at 320 °C, to keep the mass spectrometer memory as low as possible. Also, bombardment with argon ions helped in reducing memory. All isotopic ratios and ion beam intensities were measured as a function of time and all the data were extrapolated to the time of sample introduction.

Even after prolonged baking some background peaks were present at masses 76, 77 and 78, probably due to the C_6H_6 ring. A small correction, deduced from the observed 76 and 77 background, had therefore to be applied to Kr^{78}. However, this correction was always smaller than 3% and the uncertainty of the correction has been included in the error assigned to Kr^{78}. No other hydrocarbon background in the krypton and xenon mass region was present.

A broad background peak at mass 80 was observed when large amounts of Ar were introduced into the mass spectrometer. This background peak could either be due to Ar_2^+ molecules or to charge exchange ($Ar^{++} \rightarrow Ar^+$) between ion source and magnetic analyzer. At argon pressures below 10^{-7} mm Hg the mass 80 peak always disappeared, if the electron energy was reduced below the Ar^{++} appearance potential (44 V). At higher argon pressures ($> 10^{-6}$ mm Hg) the peak at mass 80 could not be eliminated by lowering the electron energy. Thus, at lower pressures only charge exchange contributes to the mass 80 peak, whereas at higher pressures also Ar_2^+ molecules are formed. However, the argon present in the Kr fraction was small enough that no corrections had to be applied. ArKr molecules could interfere with the xenon masses 124 and 126. Therefore, masses 122 and 123 were always monitored during the xenon measurements. These molecules were never observed.

4. Results

The results of our krypton and xenon measurements are given in Tables 4 and 5. For comparison the isotopic composition of atmospheric krypton

meteorite	Kr^{tot}	Kr^{86}	Kr^{78}	Kr^{80}	Kr^{82}	Kr^{83}	Kr^{84}	Kr^{86}
	10^{-12} cc STP/gm							
Abee	2550 ± 300	440	2.03 ± 0.06	17.9 ± 0.2	68.0 ± 0.6	65.7 ± 0.5	326 ± 2	100
Bruderheim	290 ± 50	47	4.28 ± 0.12	20.8 ± 0.2	76.5 ± 0.6	80.1 ± 0.6	335 ± 2	100
H-Ausson	380 ± 80	61	4.76 ± 0.16	21.8 ± 0.4	78.3 ± 0.8	82.0 ± 0.8	337 ± 3	100
Mezö-Madaras	5300 ± 800	913	2.03 ± 0.10	17.7 ± 0.4	68.1 ± 0.8	65.8 ± 0.7	327 ± 2	100
Stannern	170 ± 20	10.5	70.0 ± 0.8	199 ± 3	341 ± 5	431 ± 5	482 ± 4	100
terrestrial atmos.	—	—	2.04	13.1	66.6	66.5	327.6	100

Table 4. Concentrations and isotopic compositions of krypton in the investigated meteorites. The isotopic compositions are normalized to $Kr^{86} \equiv 100\%$. The data for terrestrial krypton are from NIER [14].

meteorite	Xe^{tot}	Xe^{132}	Xe^{124}	Xe^{126}	Xe^{128}	Xe^{129}	Xe^{130}	Xe^{131}	Xe^{132}	Xe^{134}	Xe^{136}
	10^{-12}ccSTP/gm										
Abee	4900	612	0.47	0.42	8.52	524	15.7	81.5	100	38.2	32.2
	± 250		± 0.02	± 0.02	± 0.08	± 15	± 0.1	± 0.5		± 0.2	± 0.2
Bruderheim	400	99	0.56	0.59	8.29	125.2	15.8	81.8	100	38.6	32.5
	± 35		± 0.02	± 0.02	± 0.08	± 1.0	± 0.1	± 0.5		± 0.2	± 0.2
H-Ausson	490	120	0.59	0.65	8.40	129.4	15.8	81.9	100	38.4	32.4
	± 70		± 0.02	± 0.02	± 0.10	± 2.0	± 0.1	± 0.5		± 0.2	± 0.2
Mezö-Madaras	8200	2050	0.46	0.42	8.40	124.1	15.9	81.4	100	38.0	32.0
	± 600		± 0.02	± 0.02	± 0.12	± 1.0	± 0.2	± 0.5		± 0.3	± 0.3
Stannern	115	25	7.6	12.7	23.8	98.0	23.0	108.9	100	45.0	40.4
	± 7		±0.2	± 0.2	± 0.2	± 2.0	± 0.2	± 0.7		± 0.4	± 0.4
terrestrial atmos.	—	—	0.36	0.33	7.14	98.3	15.2	78.8	100	38.8	33.0

Table 5. Concentrations and isotopic compositions of xenon in the investigated meteorites. The isotopic compositions are normalized to $Xe^{132} \equiv 100\%$. The data for terrestrial xenon are from NIER [14].

[14] A. O. NIER, Phys. Rev. **79**, 450 [1950].

meteorite	S %	Cl ppm	Ca %	Fe %	Se ppm	Br ppm	Rb ppm	Sr ppm	Y ppm	Zr ppm	Te ppm	I ppb	Ba ppm	REE ppm	U ppb
Abee	—	530[q]	1.1[a]	32.6[a]	(15)[p]	3.5[l]	—	—	1.0[m]	14[k]	2.2[b]	145[b]	1.8[e]	1.71[m]	11[c]
Bruderheim	2.4[d]	100[q]	1.3[d]	21.9[e]	—	0.3[f,l]*	—	11.2[e]	—	—	0.4[b]	15[b]*	3.4[e]	—	15[b]
H-Ausson	—	—	—	—	—	—	—	—	—	—	—	—	—	—	—
Mezö-Madaras	2.3[g]	—	1.2[g]	24.1[g]	—	—	—	—	—	—	—	—	—	—	—
Stannern	0.31	—	6.8[e]	17.5[e]	—	—	—	85[e]	28[h]	70[k]	—	—	42.2[e]	51.3[h]	—
Average hypersthene chondrites	2.22[n]	110[q]	1.36[n]	21.6[n]	9[p]	0.4[f,l]*	2.8°	11°	2.0[h,m]	11[k]	0.5[b]	35[b]*	3.4[e]	3.4[h,m]	14[c]
Average bronzite chondrites	1.93[n]	100[q]	1.27[n]	27.8[n]	9[p]	0.2[f,l]*	2.8°	11°	2.1[m]	8[k]	0.5[b]	35[b]*	3.4[e]	3.4[h,m]	14[c]

Table 6. Chemical abundances of some elements relevant to the discussion of the krypton and xenon abundance pattern. * Large variations reported.

a Kirsten, Krankowsky, and Zähringer [12]
b Goles and Anders [15]
c Reed, Kigoshi, and Turkevich [16]
d Duke, Maynes, and Brown [17]
e Wyttenbach and Dulakas [18]
f Wyttenbach, von Gunten, and Scherle [19]
g Rammelsberg [20]
h Schmitt, Smith, and Olehy [21]
i Reed [22]
k Schmitt, Bingham, and Chodos [23]
l Merrill [24]
m Schmitt, Smith, Lasch, Mosen, Olehy, and Vasilevskis [25]
n Mason [26]
o Gast [27]
p DuFresne [28]
q von Gunten, Wyttenbach, and Scherle [29]

and xenon is listed. The errors assigned to the individual values are based on the agreement obtained between the duplicate analyses of the particular meteorite. Additional factors, such as sample size, absolute rare gas concentration, uncertainty in extraction blank and correction of mass discrimination were also taken into account. The errors in our gas standards are included in the indicated concentration errors.

In Table 6 chemical abundances of some elements relevant to the discussion of the krypton and xenon results are compiled. The determinations of Wyttenbach and Dulakas [18] were made on aliquots of the samples used for the rare gas measurements.

In Table 7 our results on Bruderheim and Abee are compared with those published by other investigators. Clarke and Thode [8] report substantial variations of the krypton contents and isotopic compositions in different samples of the same meteorite. They show that this could be due to varying amounts of atmospheric contamination adsorbed or occluded in their uncrushed meteorite samples. Also their sample preheating procedure may have led to some gas losses. For the comparison we have chosen those of their results for which simultaneously the concentration and the isotopic composition are known.

Our krypton concentrations agree very well with those of Zähringer [30], whereas the values of Clarke and Thode [8] for Abee 3, 4 and Bruderheim 6

15 G. G. Goles and E. Anders, Geochim. Cosmochim. Acta **26**, 723 [1962].
16 G. W. Reed, K. Kigoshi, and A. Turkevich, Geochim. Cosmochim. Acta **20**, 122 [1960].
17 M. Duke, D. Maynes, and H. Brown, J. Geophys. Res. **66**, 3557 [1961].
18 A. Wyttenbach and H. Dulakas, private communication 1965.
19 A. Wyttenbach, H. R. von Gunten, and W. Scherle, Geochim. Cosmochim. Acta **29**, 467 [1965].
20 C. Rammelsberg, Z. Deutsch. Geol. Gesell. **23**, 734 [1871].
21 R. A. Schmitt, R. H. Smith, and D. A. Olehy, Geochim. Cosmochim. Acta **28**, 67 [1964].
22 G. W. Reed, private communication 1965.
23 R. A. Schmitt, E. Bingham, and A. A. Chodos, Geochim. Cosmochim. Acta **28**, 1961 [1964].
24 G. Merrill, Mem. Nat. Acad. Sci. **14**, 22 [1925].
25 R. A. Schmitt, R. H. Smith, J. E. Lasch, A. W. Mosen, D. A. Olehy, and J. Vasilevskis, Geochim. Cosmochim. Acta **27**, 577 [1963].
26 B. Mason, Am. Museum Novitates No. **2223** [1965].
27 P. W. Gast, J. Geophys. Res. **65**, 1287 [1960].
28 A. DuFresne, Geochim. Cosmochim. Acta **20**, 141 [1960].
29 H. R. von Gunten, A. Wyttenbach, and W. Scherle, Geochim. Cosmochim. Acta **29**, 475 [1965].
30 J. Zähringer, Z. Naturforschg. **17 a**, 460 [1962].

meteorite	reference	Kr^{84} $\times 10^{-12}$ ccSTP/gm	Kr^{78}	Kr^{80}	Kr^{82}	Kr^{83}	Kr^{84}	Kr^{86}
Abee	a	1430	2.03	17.9	68.0	65.7	326	100
Abee 3	b	850	2.01	18.7	68.1	66.1	325	100
Abee 4	b	560	2.09	20.5	69.9	67.2	328	100
Abee	c	1500	—	—	—	—	—	—
Bruderheim	a	157	4.28	20.8	76.5	80.1	335	100
Bruderheim 4	b	160	2.72	15.2	71.6	72.5	332	100
Bruderheim 6	b	16	6.56	27.2	87.7	94.0	347	100
Bruderheim	c	150	—	—	—	—	—	—

meteorite	reference	Xe^{132} $\times 10^{-12}$ ccSTP/gm	Xe^{124}	Xe^{126}	Xe^{128}	Xe^{129}	Xe^{130}	Xe^{131}	Xe^{132}	Xe^{134}	Xe^{136}
Abee	a	610	0.47	0.42	8.52	524	15.7	81.5	100	38.2	32.2
Abee	d	820	0.40	0.36	8.82	636	16.1	81.0	100	38.1	32.0
Abee	c	800	—	—	—	640	—	—	100	—	—
Abee	e	—	—	—	—	530	—	—	100	—	—
Bruderheim	a	99	0.56	0.59	8.29	125.2	15.8	81.8	100	38.6	32.5
Bruderheim	d	250	0.50	0.52	11.7	119.6	16.2	80.4	100	39.2	33.3
Bruderheim	c	130	—	—	—	130	—	—	100	—	—

Table 7. Comparison of our results with published data. References: [a] Present work; [b] CLARKE and THODE [8]; [c] ZÄHRINGER [30]; [d] CLARKE and THODE [6]; [e] JEFFERY and REYNOLDS [31].

are much lower. The isotopic composition of Abee 3 agrees with our results, but Abee 4 shows larger $Kr^{80, 82}$ anomalies. The anomalies in our Bruderheim sample lie between those observed for Bruderheim 4 and 6. The spallation spectra derived from our Bruderheim sample and from Bruderheim 6 are in good agreement with each other (cf. Figure 5).

The agreement between the published xenon concentrations and our results is satisfactory for Abee. In Bruderheim CLARKE and THODE [6] find a 2.5 times higher xenon concentration; the deviation between our and ZÄHRINGER's [30] values lies within the experimental errors. The isotopic composition of the heavier xenon isotopes agrees better for Abee than for Bruderheim. Differences of up to 15% occure for Xe^{124} and Xe^{126} and even more for Xe^{128} of Bruderheim.

5. General Discussion

REYNOLDS and co-workers [1–5] distinguish between the "special anomaly" in the relative abundance of meteoritic Xe^{129} due to radioactive decay of extinct I^{129} and the "general anomalies" which affect the whole spectrum of meteoritic xenon. Krypton had been investigated to a lesser extent until now, and therefore, the general anomalies in its isotopic composition were not as well known. The purpose of the present work is to study the general anomalies of krypton and xenon. Thus, we shall not further discuss the Xe^{129} isotope in our samples.

The following processes may have contributed to the general anomalies of meteoritic krypton and xenon:

1. Mass fractionation due to gravitational, electrostatic or electromagnetic forces (KRUMMENACHER, MERRIHUE, PEPIN and REYNOLDS [2]).
2. Spallation and (n,γ) reactions induced by the exposure of the meteorite to the cosmic radiation during its recent history (MERRIHUE [4]; CLARKE and THODE [8]).
3. In situ production in meteoritic constituents by particle irradiation or spontaneous fission during the early history of the solar system (GOLES and ANDERS [32]; ROWE and KURODA [7]).
4. Addition of products from particle irradiation or fission to the "primordial" Kr and Xe before it became trapped in the meteorite.

It is of course important to remember that not only meteoritic krypton and xenon may have been changed, but that also the isotopic composition of ter-

[31] P. M. JEFFERY and J. H. REYNOLDS, Z. Naturforschg. **16a**, 431 [1961].

[32] G. G. GOLES and E. ANDERS, J. Geophys. Res. **66**, 889 [1961].

restrial krypton and xenon may have been altered by some of these processes (KURODA [33]; CAMERON [34]). In the cases 3 and 4 a multitude of possible reactions has to be considered:

a) Spallation reactions,
b) Special nuclear reactions on Se, Rb, Sr, Te, Cs, Ba etc.,
c) (n,γ) reactions,
d) Spontaneous fission of U^{238} or transuranium elements,
e) Neutron induced fission.

Obviously the effects of such a large number of conceivable processes can only be distinguished with great effort. REYNOLDS and co-workers have successfully applied the method of stepwise heating to establish a number of relations governing the general anomalies of the isotopic abundances of xenon. We have chosen here a different approach and have analyzed selected meteorites, where some of the processes leading to anomalies are strongly enhanced.

6. Spallation Produced Isotopes of Krypton and Xenon

6.1 The Stannern Achondrite

In Figs. 1 and 2 the measured mass spectra of krypton and xenon from the Stannern achondrite are reproduced. As these are original spectra,

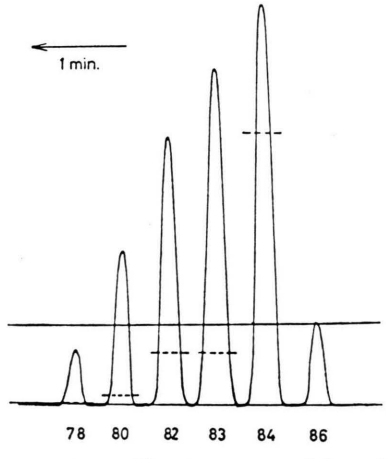

Fig. 1. Mass spectrum of krypton extracted from the Stannern achondrite (original tracing). All isotopes are measured with the same sensitivity. The solid line indicates the decrease of the ion beam intensity with time. The dashed lines correspond to the isotopic composition of atmospheric krypton arbitrarily normalized at Kr^{86}. Increased scanning speed between the peaks was used. The Kr^{86} peak corresponds to 25×10^{-12} cc STP.

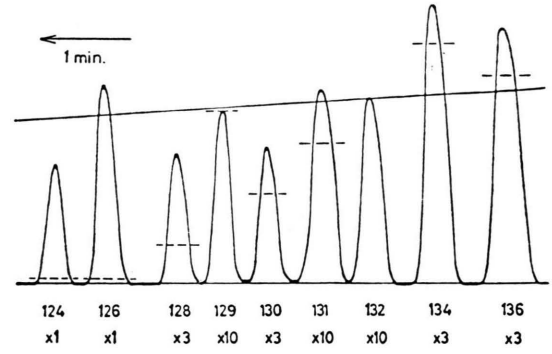

Fig. 2. Mass spectrum of xenon extracted from the Stannern achondrite (original tracing). Scaling factors are indicated below the mass number. The solid line indicates the decrease of the ion beam intensity with time. The dashed lines correspond to the isotopic composition of atmospheric xenon, arbitrarily normalized at Xe^{132}. Increased scanning speed between the peaks was used. The Xe^{124} peak corresponds to 1.5×10^{-12} cc STP.

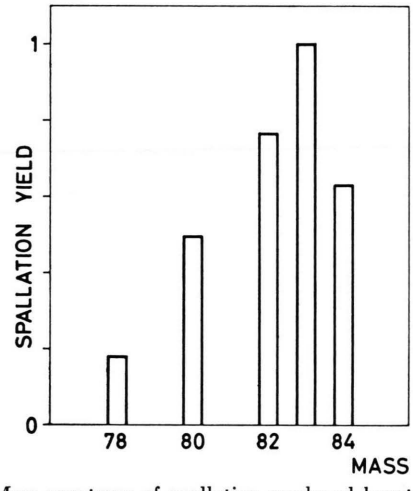

Fig. 3. Mass spectrum of spallation produced krypton as derived from the Stannern meteorite, normalized to $Kr_S^{83}{}_{all} = 1$. For errors see Table 8.

no corrections for blank or discrimination have been applied. The large enrichment of the light Xe and Kr isotopes in this meteorite is evidently due to spallation. It results from a combination of three favorable factors: high abundances of the elements Sr, Y, Zr, Ba, and rare earths which have large spallation cross sections for the production of Kr and Xe isotopes; a relatively high radiation age; and very low abundances of trapped Kr and Xe. Similar, but much smaller enrichments of the light isotopes of Kr and Xe are observed in the H-Ausson and Bruderheim chondrites. In Figs. 3 and 4 and

[33] P. K. KURODA, Nature **187**, 36 [1960].

[34] A. G. W. CAMERON, Icarus **1**, 13 [1962].

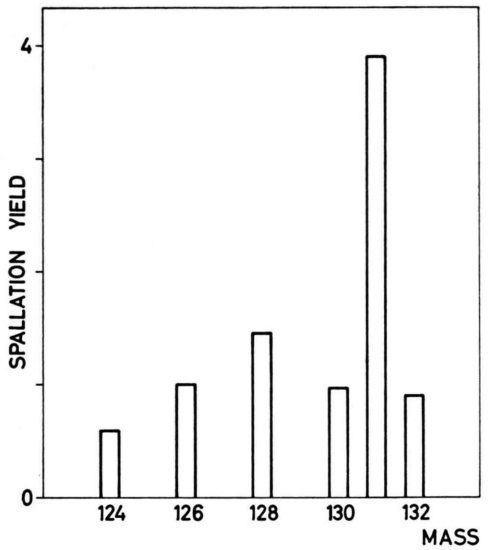

Fig. 4. Mass spectrum of spallation produced xenon as derived from the Stannern meteorite, normalized to $Xe^{126}_{spall} = 1$. For errors see Table 8.

Table 8 the mass spectra of spallation produced Kr and Xe are given. They were calculated from the observed isotopic composition in Stannern with the following considerations:

1. It is assumed that in the Stannern achondrite Xe and Kr consist essentially of three components: spallation, fission and trapped gases. The mixing ratio of these components is unknown and has to be determined.

2. The spallation spectra are unknown. However, it can be assumed that Xe^{136}_{spall} is practically zero, and $(Kr^{86}/Kr^{83})_{spall} \leqq 0.1$. In fact, radiochemical studies of spallation reactions on yttrium, iodine, caesium etc. [35–40] show that spallation products from heavier elements have strong neutron deficiencies. Isotopes occupying similar positions as Xe^{136} or Kr^{86} are hardly produced at all. This tendency becomes more pronounced with growing Z, showing the effect of the rising Coulomb barrier. The resulting low spallation yield for Xe^{134} (cf. Table 8) in fact confirms that the Xe^{136} yield must be very low.

3. The isotopic composition of fission xenon can, of course, not be deduced from the measured xenon spectrum in Stannern, as it is masked by the large and unknown spallation contribution. We may, however, assume that the spectra of the fission components in the Stannern and Pasamonte meteorites are identical. Both are calcium-rich achondrites, but with different radiation ages. Rowe and Kuroda [7] have recently measured the xenon spectrum in Pasamonte and have derived a fission spectrum. They have, however, neglected the spallation component which is much smaller than that in Stannern, but still significant. As the authors do not give Xe^{124} and Xe^{126} abundances the spallation component has to be calculated either from the Xe^{128}/Xe^{130} ratio or from the known radiation age of Pasamonte (cf. chapter 7).

The correction for fission Kr is small and uncertainties in the Kr fission spectrum have little influence on the Kr spallation spectrum. Wetherill's [41] data for the spontaneous fission of U^{238} were taken.

4. For the correction of the trapped gas component, the isotopic composition of Kr and Xe measured in the Mezö-Madaras meteorite was taken. As will be discussed later, Kr^{80}, and to a lesser extent Kr^{82} and Xe^{128} are enriched by (n,γ) reactions in this meteorite relative to carbonaceous chondrites. For these three isotopes the average carbonaceous chondrite abundances were used.

5. The mixing ratio of trapped Xe to fission Xe in Stannern can be derived from the measured Xe^{134}/Xe^{136} ratio. As this ratio is similar in the fission and in the trapped gas component, only rather wide limits for the mixing ratio are obtained. Taking experimenal errors into account and assuming that fission Xe in Stannern and Pasamonte has the same iso-

		Kr^{78}	Kr^{80}	Kr^{82}	Kr^{83}	Kr^{84}		
		0.179 ± 0.008	0.495 ± 0.020	0.765 ± 0.025	1.00	0.63 ± 0.17		
Xe^{124}	Xe^{126}	Xe^{128}	Xe^{130}	Xe^{131}	Xe^{132}	Xe^{134}	$\frac{Xe^{128}}{Xe^{130}}$	$\frac{Xe^{131}}{Xe^{130}}$
0.590 ± 0.015	1.00	1.45 + 0.25 − 0.12	0.97 + 0.50 − 0.25	3.9 + 2.5 − 1.1	0.9 + 2.3 − 0.9	≦ 0.25	1.50 ± 0.35	4.0 ± 0.2

Table 8. Isotopic composition of spallation produced krypton and xenon as derived from the Stannern meteorite.

[35] J. M. Miller and J. Hudis, Ann. Rev. Nucl. Sci. **9**, 159 [1959].
[36] B. G. Harvey, in Progress in Nuclear Physics (O. R. Frisch ed.), Pergamon Press, London 1959, p. 89.
[37] A. A. Caretto and E. O. Wiig, Phys. Rev. **103**, 236 [1956].
[38] J. H. Coleman and H. A. Tewes, Phys. Rev. **99**, 288 [1955].
[39] R. W. Fink and E. O. Wiig, Phys. Rev. **96**, 185 [1954].
[40] L. Winsberg, Phys. Rev. **95**, 198 [1954].
[41] G. W. Wetherill, Phys. Rev. **92**, 907 [1953].

topic composition, one obtains $0.3 \leqq Xe^{136}_{fission}/Xe^{136} \leqq 1$. A better upper limit for the $Xe^{136}_{fission}$ content can be obtained from the concentration of trapped krypton. A survey of all the available data on trapped gases shows that trapped Xe in most meteorites is more abundant than trapped Kr (PEPIN and SIGNER [42, 43]). In meteorites with solar-type trapped gases the lowest $(Xe/Kr)_{trapped}$ ratio observed is 0.3. No indication for solar type trapped gases is found in Stannern. For planetary-type trapped gases the lowest $(Xe/Kr)_{trapped}$ ratio observed is 0.7. Using this figure as lower limit for Stannern, one obtains $Xe^{136}_{fission}/Xe^{136} \leqq 0.8$. An upper limit for $Kr^{86}_{fission}/Kr^{86}$ of 0.12 in Stannern is obtained from the Kr/Xe ratio of U^{238} spontaneous fission [41]. If the fission component in Stannern had resulted from spontaneous fission of transuranium elements, the fission ratio Kr/Xe would probably be smaller. Thus, $Kr^{86}_{fission}/Kr^{86} \leqq 0.12$ is assumed.

It should be pointed out that the relative spallation production rates of the *light* isotopes of Kr and Xe are quite independent of all these assumptions. This is reflected in their small errors. Especially the Xe^{126}/Xe^{124} ratio is virtually not influenced by any possible correction.

Xe^{130} has a relatively low spallation yield. This is due to partial shielding by Ba^{130} and reflects the strong neutron deficiency in heavy spallation products.

6.2 *Spallation Isotopes in Chondrites*

The Kr and Xe spallation components in the chondrites H-Ausson and Bruderheim can be deduced in the same way. For xenon only Xe^{124}_{spall} and Xe^{126}_{spall} can be determined with sufficient accuracy. We have corrected these two isotopes with the Xe composition of Mezö-Madaras.

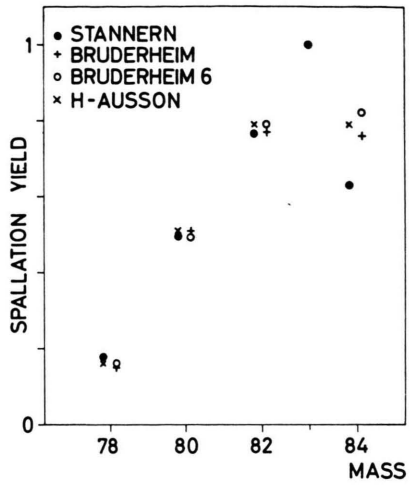

Fig. 5. Comparison of the mass spectra of spallation krypton in three meteorites. Bruderheim 6 from CLARKE and THODE [8], all the others from the present work.

$(Xe^{124}/Xe^{126})_{spall}$ ratios are given in Table 9. The agreement between the three meteorites is very good.

A comparison between the Kr spallation spectra in Stannern, H-Ausson and Bruderheim is given in Fig. 5. The average isotopic composition of krypton from carbonaceous chondrites was assumed for the correction for trapped krypton. Included is also a spallation spectrum derived from the Kr anlysis of Bruderheim 6 by CLARKE and THODE [8]. The agreement is generally good.

In Table 9 the concentrations of some spallation isotopes of argon, krypton and xenon are compared. It is evident that the concentrations of the Xe and Kr spallation isotopes rise with increasing radiation

meteorite	radiation age 10^6 yrs.	Ar^{38}_{spall} 10^{-8} cc/gm	Kr^{82}_{spall} 10^{-12} cc/gm	Xe^{126}_{spall} 10^{-12} cc/gm	$\left(\frac{Xe^{126}}{Ar^{38}}\right)_{spall}$	$\left(\frac{Xe^{126}}{Kr^{82}}\right)_{spall}$	$\left(\frac{Xe^{126}}{Xe^{124}}\right)_{spall}$
H-Ausson	50	3.1[a]	8.5	0.30	1.0×10^{-5}	0.035	1.7
Bruderheim	26	1.44[a]	5.7	0.19	1.3×10^{-5}	0.033	1.65
Average chondrite, spallation theory					2.6×10^{-5}	0.058	
Stannern	~ 30	5.15[b]	31	3.1	6×10^{-5}	0.10	1.70 ± 0.05
Stannern, spallation theory					12×10^{-5}	0.11	

Table 9. Concentrations of some spallation produced isotopes in three meteorites. Concentrations of the other spallation isotopes can be calculated from ratios given in Table 8. For comparison ratios of spallation isotopes calculated from general spallation theory [Eq. (3)] are given. References: [a] EBERHARDT, EUGSTER, GEISS, and MARTI [13]; [b] KIRSTEN, KRANKOWSKY, and ZÄHRINGER [12].

[42] R. O. PEPIN and P. SIGNER, Science **149**, 253 [1965].

[43] Contrary to PEPIN and SIGNER [42], we assume that the excess Xe^{129} does not belong to the trapped component.

age. The higher concentrations in Stannern reflect the greater abundances of Sr, Zr, Ba, and the rare earth elements in this meteorite. This pattern strongly suggests that the spallation components of Xe and Kr in the three meteorites were produced by the same radiation as were He^3, Ne^{21} and Ar^{38}, i. e. they are due to cosmic ray bombardment late in the history of the solar system. In the following this will be discussed in a more quantitative way.

6.3 Comparison between Observed and Calculated Spallation Yields

The excitation function for spallation reactions can be approximated by [44–46]

$$\sigma(E, A_0, \Delta A) = \sigma_0 A_0^{2/3} c E^{-2/3} \exp[-c E^{-2/3} \Delta A] \quad (1)$$

with $$c = \frac{0.25}{1+0.022 A_0} \text{GeV}^{2/3}, \quad \sigma_0 = 60 \text{ mb}.$$

A_0 is the atomic number of the target nucleus and ΔA the total mass loss. Assuming an irradiation spectrum of the form

$$f(E)\, dE = f_0 E^{-\alpha}\, dE \quad (2)$$

and upon integrating, one obtains for the production rate of an isobar [47]

$$P(\Delta A, A_0) = B \cdot (\Delta A)^{-n} \quad (3)$$

with $B = \frac{3}{2} \sigma_0 A_0^{2/3} f_0 \Gamma(n)/c^{n-1}$, $n = \frac{1}{2}(3\alpha - 1)$.

Equation (3) has been successfully applied to iron meteorites with Fe as target [47, 48], as well as to other target elements in meteorites [49]. The parameter n depends on the hardness of the irradiation and can be calculated if the ΔA distribution of spallation isotopes has been measured. Values of $n = 2.0$ for small iron meteorites rising to $n = 2.6$ for large ones have been obtained [47, 48, 50]. No experimental data exist for stone meteorites. However, most stone meteorites are small and we have chosen $n = 2$ for all three meteorites.

$P(\Delta A, A_0)$ is the production rate for the total isobar. It has to be multiplied by the isobaric fraction coefficient g in order to obtain the cross section for one nucleus. We shall explicitly calculate production rates for Ar^{38}, Kr^{82} and Xe^{126}. For Ar^{38} and Kr^{82} $g = 1$. For Xe^{126} $g = 0.8$ is estimated from radiochemical spallation data [35–40].

Equation (3) has to be summed over all target nuclei in the meteorite. The chemical abundances given in Table 6 are used. Ar^{38} is mainly produced from Ca and Fe; Kr^{82} from Sr, Zr and Y; and Xe^{126} from Ba and the rare earth elements.

The spallation formula (3) breaks down for $\Delta A \lesssim 5$, i. e. for $Rb \rightarrow Kr^{82}$ and $Ca \rightarrow Ar^{38}$. We therefore take

$$\sigma(Ca \rightarrow Ar^{38}) = 11.8 \times \sigma(Fe \rightarrow Ar^{38})$$

from Stauffer's [11] work and assume

$$\sigma(Rb \rightarrow Kr^{82}) = \sigma(Sr \rightarrow Kr^{82}).$$

Production rates calculated from Eq. (3) are given in Table 9. They are estimated to be correct only within a factor of two, in view of the wide range in A_0 and ΔA to which the very simple spallation formula (3) is being applied. Thus, the agreement between experimentally observed and theoretical ratios of spallation isotopes is quite satisfactory.

For practical purposes the production rates of Ar^{38}, Kr^{83} and Xe^{126} can be approximately calculated from the simple relations

$$Ar^{38}_{spall} = \varkappa T_r([Fe] + a[Ca]), \quad (4)$$

$$Kr^{83}_{spall} = \varkappa T_r(b[Sr] + c[Y] + d[Zr]), \quad (5)$$

$$Xe^{126}_{spall} = \varkappa T_r(e[Ba] + f[REE]), \quad (6)$$

and

$$\left(\frac{Xe^{126}}{Ar^{38}}\right)_{spall} = \frac{e[Ba]+f[REE]}{[Fe]+a[Ca]}, \quad (7)$$

$$\left(\frac{Xe^{126}}{Kr^{83}}\right)_{spall} = \frac{e[Ba]+f[REE]}{b[Sr]+c[Y]+d[Zr]} \quad (8)$$

with
$a = 16.5$, $d = 3.2$,
$b = 10$, $e = 1.25$,
$c = 5.9$, $f = 0.45$,
$\varkappa = 0.12 \times 10^{-8}$ cc STP/m. y. gm

T_r : radiation age,
[Fe] = concentrations of Fe + Ni + Co + Mn + Cr + V,
[Ca] = concentrations of Ca + K + Sc + Ti,
[Sr] = concentrations of Sr + Rb,
[Y] = concentration of Y,
[Zr] = concentrations of Zr + Nb + Mo,
[Ba] = concentrations of Ba + Cs,
[REE] = concentrations of elements La to Lu.

[44] G. Rudstam, Thesis, University of Uppsala 1956.
[45] M. Honda and D. Lal, Phys. Rev. **118**, 1618 [1960].
[46] H. Oeschger and U. Schwarz, unpublished calculations, 1961.
[47] J. Geiss, H. Oeschger, and U. Schwarz, Space Sci. Rev. **1**, 197 [1962].
[48] H. Stauffer and M. Honda, J. Geophys. Res. **67**, 3503 [1962].
[49] F. Begemann, Z. Naturforschg. **20 a**, 950 [1965].
[50] H. Voshage, Z. Naturforschg. **17 a**, 422 [1962].

meteorite	Xe^{126}_{spall}		$(Xe^{126}/Ar^{38})_{spall}$		$(Xe^{126}/Kr^{83})_{spall}$	
	measured 10^{-12} cc/gm	Eq. (6) 10^{-12} cc/gm	measured 10^{-5}	Eq. (7) 10^{-5}	measured	Eq. (8)
Bruderheim	0.19	0.18	1.32	1.22	0.026	0.031
H-Ausson	0.30	0.35	0.97	1.11	0.028	0.032
Stannern	3.1	2.7	6.0	5.7	0.077	0.061

Table 10. Comparison of measured Xe^{126}_{spall} concentrations and $(Xe^{126}/Ar^{38})_{spall}$ and $(Xe^{126}/Kr^{83})_{spall}$ ratios with figures calculated according to Eqs. (6), (7), and (8).

The value for a is taken from STAUFFER [11]; $c/b = 0.59$, $d/b = 0.32$, and $f/e = 0.36$ are calculated from Eq. (3), b and e are averages obtained from the observed $(Xe^{126}/Ar^{38})_{spall}$ and $(Xe^{126}/Kr^{83})_{spall}$ ratios in H-Ausson, Bruderheim and Stannern. $\varkappa$ is based on H^3/He^3 radiation ages and He^3/Ar^{38}_{spall} ratios [13]. Variations in the size of the meteorite should influence Eqs. (7) and (8) less than Eqs. (4), (5), and (6).

In Table 10 Xe^{126}_{spall} concentrations and $(Xe^{126}/Ar^{38})_{spall}$ and $(Xe^{126}/Kr^{83})_{spall}$ ratios calculated from Eqs. (6), (7) and (8) are compared with the measured values. The agreement is satisfactory.

6.4 Conclusions

All these observations on the Kr and Xe spallation fractions in the three meteorites H-Ausson, Bruderheim and Stannern can be summarized as follows:

1. The spectra obtained are typical for spallation products from heavy elements.
2. The concentrations are proportional to radiation ages.
3. The concentrations vary according to chemical abundances.
4. The production rates are in agreement with general spallation theory.

We may, thus, safely accept that the irradiation responsible for the production of Ar^{38}_{spall}, Ne^{21}_{spall} and He^3_{spall} can fully account for the Kr and Xe spallation components observed in the three meteorites. It is generally agreed that the light spallation isotopes have been produced by cosmic radiation after the meteorite was removed from a shielded location inside its parent body late in its history. Consequently, this is also true for spallation Xe and Kr observed in the three meteorites discussed here.

A survey of the literature shows that *so far* all the observed Xe^{124} and Xe^{126} anomalies, which are higher than the carbonaceous chondrite abundances, can be interpreted as arising from a mixture of

a) primordial Xe as observed in carbonaceous chondrites; and
b) spallation xenon produced by cosmic radiation late in the history of the meteorite.

Until now the most extreme Xe^{124} and Xe^{126} anomalies were those observed by MERRIHUE [4] in separated chondrules of Bruderheim. The Xe^{126} excess, when corrected for meteoritic trapped xenon, is 0.2×10^{-12} cc STP/gm, which is very close to our figure of 0.19×10^{-12}cc STP/gm observed in the whole meteorite (Table 9).

7. Fission Xenon

ROWE and KURODA [7] have found a fission component in the Pasamonte achondrite, corresponding to $Xe^{136}_{fission} = 3 \times 10^{-12}$ cc STP/gm. In Stannern a similar fission component is detectable. However, because of the larger concentration of spallation isotopes the fission component can only be determined approximately in this meteorite. As outlined in chapter 6.1, $Xe^{136}_{fission}$ in Stannern lies between 3 and 8×10^{-12} cc STP/gm. If the xenon in the chondrites H-Ausson and Bruderheim is compared with that in Mezö-Madaras or other meteorites containing large amounts of Xe, it is evident that the excess fission component, if at all present, is about one order of magnitude smaller. Thus, a correlation of this component with U is apparent. As pointed out by ROWE and KURODA [7], however, spontaneous fission of U^{238} cannot account for the observed fission xenon concentrations in calcium-rich achondrites by one order of magnitude, and spontaneous fission of extinct transuranium isotopes, such as Pu^{244} ($T_{1/2} = 75$ m. y.), is implied. The correlation with the uranium content would then result from the geochemical affinity of U and Pu.

Rowe and Kuroda [7] have derived a spectrum for the fission xenon in Pasamonte neglecting, however, the spallation component. Even for the short radiation age of Pasamonte this introduces an appreciable error and we have recalculated the xenon fission spectrum in this meteorite using the spallation spectrum obtained in this paper. The Xe^{124} and Xe^{126} abundances are not known for Pasamonte. Therefore, the spallation contribution has to be calculated from the radiation age [52, 53] [applying Eq. (6)] or from the observed Xe^{128}/Xe^{130} ratio. Both methods give virtually the same fission spectrum. The choice of the isotopic composition for the trapped component is not critical. Correcting with either average carbonaceous chondrite (AVCC [2]) xenon or terrestrial xenon leads to very similar xenon fission spectra as can be seen from Fig. 6. The indicated errors include the experimental errors as well as the uncertainties in the spallation concentration and spectrum.

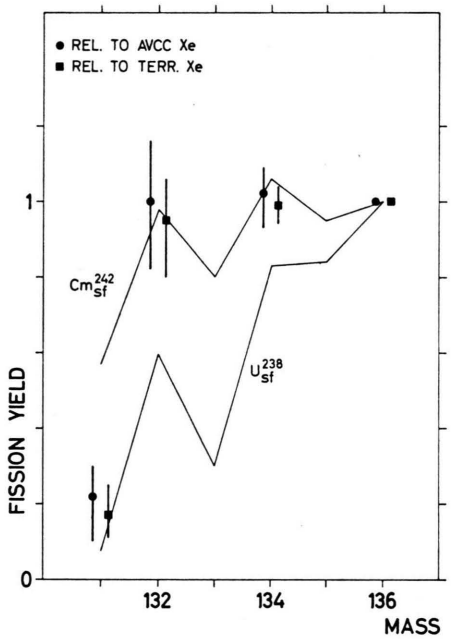

Fig. 6. Mass spectrum of fission xenon as derived from Rowe and Kuroda's [7] measurement of the Pasamonte achondrite. The spallation component has been corrected for. $Xe^{130}_{fission}$ was assumed to be zero. Solid circles: AVCC−Xe isotopic composition assumed for the trapped component (relative fission yields $Xe^{136}=1.00$; $Xe^{134}=1.02^{+0.07}_{-0.09}$; $Xe^{132}=1.00^{+0.16}_{-0.18}$; $Xe^{131}=0.22^{+0.08}_{-0.12}$). Solid squares: terrestrial xenon isotopic composition assumed for the trapped component (reraltive fission yields $Xe^{136}=1.00$; $Xe^{134}=0.99\pm0.05$; $Xe^{132}=0.95^{+0.11}_{-0.15}$; $Xe^{131}=0.17^{+0.08}_{-0.06}$). For comparison the spontaneous fission yield curves for U^{238} and Cm^{242} are given [51].

The xenon fission spectrum obtained from Pasamonte is different from that of U^{238} and Cf^{252} spontaneous fission, and also of U^{235} slow neutron induced fission [51]. The high yield for mass 132 is in agreement with the Cm^{242} yield curve. A high Xe^{132} spontaneous fission yield is also expected from 75 m. y. Pu^{244} because of the influence of double magic Sn^{132} (Cameron [34]).

The spectrum we obtain for meteoritic fission xenon is remarkably similar to that in the Navajo natural gas [6].

8. Trapped Gases

8.1 Trapped Xenon

The isotopic composition of xenon in meteorites containing large quantities of heavy noble gases is listed in Table 11. The AVCC (average carbonaceous chondrite) figures are averages from analyses of Murray, Mighei, and Orgueil [2]. Enstatite chondrites not listed (Indarch, St. Mark's [2]) have Xe isotopic ratios similar to Abee. Reynolds and Turner [54] have extensively studied Xe in the Renazzo chondrite and have shown that it contains at least three components. They may be described as follows:

1. Xe evolved at 200 – 400 °C having an isotopic composition somewhere between carbonaceous chondrites and the atmosphere.
2. Xe released at 500 – 1300 °C having an isotopic composition close to that of carbonaceous chondrites.
3. Fission xenon.

The component 3. is included in the 500 – 1300 °C fraction in Table 11. Because of the rather high abundance of the low temperature component Reynolds and Turner [54] have concluded that its isotopic composition cannot be explained by terrestrial contamination. It is interesting to speculate that part of this component might be "solar type" trapped gas, whereas Xe released at higher temperature

[52] J. Geiss and D. C. Hess, Astrophys. J. **127**, 224 [1958].
[53] P. Eberhardt and D. C. Hess, Astrophys. J. **131**, 38 [1960].
[51] E. K. Hyde, Lawrence Radiation Laboratory Report No. 9036 [1960].
[54] J. H. Reynolds and G. Turner, J. Geophys. Res. **69**, 3263 [1964].

meteorite	Xe^{132} 10^{-12} ccSTP/gm	Xe^{124}	Xe^{126}	Xe^{128}	Xe^{130}	Xe^{131}	Xe^{132}	Xe^{134}	Xe^{136}
Atmosphere[a]		0.357	0.335	7.14	15.2	78.8	100	38.8	33.0
AVCC[b]		0.486	0.439	8.30	16.2	82.0	100	38.2	32.2
Renazzo[c] 200—400 °C	830	0.39	0.35	7.47	15.5	79.7	100	38.5	32.6
500—1300 °C	2600	0.464	0.413	8.20	16.3	81.9	100	38.4	32.5
Mezö-Madaras[d]	2050	0.455	0.411	8.39	15.9	81.4	100	38.0	32.0
Abee[d]	612	0.468	0.416	8.51	15.7	81.5	100	38.2	32.2

Table 11. Xe isotopic composition of xenon-rich meteorites (AVCC=average carbonaceous chondrites). Mezö-Madaras and Abee have been corrected for cosmic ray induced spallation. Data from: [a] NIER [14]; [b] KRUMMENACHER, MERRIHUE, PEPIN, and REYNOLDS [2]; [c] REYNOLDS and TURNER [54]; [d] Present work.

	Xe^{124}	Xe^{126}	Xe^{128}	Xe^{130}	Xe^{131}	Xe^{132}	Xe^{134}	Xe^{136}
Atmosphere	1.00	0.94	20.0	42.6	231	280	108.7	92.4
AVCC	1.00	0.90	17.1	33.3	169	206	78.6	66.3
17% Atm. + 83% AVCC	1.00	0.91	17.6	34.9	178	219	83.7	70.7
Mezö-Madaras	1.00	0.90	18.4	34.9	179	220	83.5	70.3
8% Atm. + 92% AVCC	1.00	0.90	17.3	34.0	173	212	81.0	68.4
Abee	1.00	0.89	18.2	33.6	174	214	81.6	68.8

Table 12. Comparison of xenon isotopic composition (corrected for spallation) of Mezö-Madaras and Abee with mixtures of AVCC and atmospheric xenon. Normalization to Xe^{124} is used (c. f. chapter 8.2). The agreement is satisfactory except for Xe^{128}, where an excess due to $I^{127}(n,\gamma\beta)Xe^{128}$ is observed in both meteorites.

constitutes the "planetary type". This would be consistent with the observation that solar type trapped gases are located at the surfaces of the individual grains in the meteorite [55–57].

Also the trapped xenon in Mezö-Madaras and Abee seems to be a mixture of AVCC-xenon and xenon of atmospheric composition as can be seen from Table 12. The agreement between the assumed mixtures and the trapped xenon is well within the experimental errors, except for an excess of Xe^{128}. This excess will be discussed in chapter 9.

8.2 Atmospheric and Meteoritic Xenon

Several possible mechanisms have been suggested in order to explain the large differences between the isotopic composition of atmospheric xenon and AVCC-xenon: 1) Trapped xenon in meteorites contains a spallation fraction [32]; 2) Mass fractionation and addition of fission xenon to meteoritic xenon [2]; 3) Nuclear reactions on Te [2]; 4) Addition of fission xenon [33] and (n,γ) products to atmospheric xenon [34]; 5) Mass fractionation in the terrestrial atmosphere.

We have shown in chapter 6.1 that in cosmic ray induced spallation the Xe^{126}/Xe^{124} ratio is 1.70 ± 0.05. This ratio will increase if spallation is induced by particles of lower energy. It might decrease somewhat if the effective irradiation energy is higher than it was in the Stannern meteorite. A large decrease, however, cannot be expected. In order to explain the difference between atmospheric and AVCC-xenon solely by the addition of a spallation fraction to the latter, a ratio $(Xe^{126}/Xe^{124})_{spall} = 0.8 \pm 0.2$ would be required. This seems to be ruled out by our observation on Stannern. Reactions of deuterons on Te give small yields for Xe^{124} and cannot be used as an explanation for the difference between atmospheric and meteoritic Xe [2]. α-particle reactions may still be a possibility, and also of course mass fractionation. But at present it seems reasonable to assume that the light Xe isotopes Xe^{124} and Xe^{126} have been affected relatively little by nuclear reactions or transformations and therefore can be useful for normalization (cf. Table 12).

9. The Kr^{80}, Kr^{82}, and Xe^{128} Anomalies

Table 13 gives a comparison of the krypton isotopic composition of meteorites with large quantities

[55] P. EBERHARDT, J. GEISS, and N. GRÖGLER, Tschermaks Mineral. Petrogr. Mitt., 3. Folge, **10**, 535 [1965].

[56] H. HINTENBERGER, E. VILCSEK, and H. WÄNKE, Z. Naturforschg. **20 a**, 939 [1965].

[57] P. EBERHARDT, J. GEISS, and N. GRÖGLER, J. Geophys. Res. **70**, 4375 [1965].

meteorite	Kr 10^{-12} ccSTP/gm	Kr^{78}	Kr^{80}	Kr^{82}	Kr^{83}	Kr^{84}	Kr^{86}
Atmosphere[a]		2.04	13.1	66.6	66.5	327.6	100
Orgueil[b]	9000	—	12.9 ± 0.2	65.0 ± 0.7	65.3 ± 0.8	323 ± 2	100
Murray[b]	7000	2 ± 0.2	12.9 ± 0.2	65.2 ± 1.0	65.5 ± 1.0	326 ± 5	100
AVCC		2	12.9	65.1	65.4	324	100
Abee 3[c]	1500	1.91 ± 0.06	18.4 ± 0.4	67.7 ± 0.5	65.5 ± 0.6	325 ± 3	100
Abee 4[c]	1000	1.94 ± 0.12	20.1 ± 0.5	69.3 ± 1.3	66.3 ± 1.3	327 ± 3	100
Abee[d]	2550 ± 300	1.97 ± 0.06	17.7 ± 0.2	67.8 ± 0.6	65.4 ± 0.5	326 ± 2	100
Mezö-Madaras[d]	5300 ± 800	1.88 ± 0.10	17.3 ± 0.2	67.5 ± 0.8	65.0 ± 0.7	326 ± 2	100

Table 13. Kr isotopic composition (corrected for spallation) in meteorites with large amounts of trapped heavy noble gases. AVCC: average carbonaceous chondrite (weighted average from Murray and Orgueil). References: [a] Nier [14]; [b] Krummenacher, Merrihue, Pepin, and Reynolds [2]; concentration from Zähringer[30]; [c] Clarke and Thode [8]; [d] Present work.

of trapped heavy noble gases. Listed are all analyses in which at least one of the two light isotopes Kr^{78} and Kr^{80} has been measured. The AVVC-krypton (weighted average from Murray and Orgueil) is identical within the limits of error with terrestrial krypton, except for a possible slight excess of Kr^{86} (Krummenacher et al. [2]). The most conspicious feature, however, is the large difference in the Kr^{80} abundance between the carbonaceous chondrites, on one hand, and Mezö-Madaras and Abee on the other. This cannot be due to spallation reactions because of the very different nature of the krypton spallation spectrum (cf. Fig. 3). Clarke and Thode [8] have already pointed out that neutron capture by bromine is the most likely explanation. This could have occurred either in situ by the meteoritic bromine or by bromine not associated with the meteorite. In the latter case the krypton formed would have been added to the trapped krypton found in the meteorite.

For the discussion of the origin of this Kr^{80} excess and the possibility of an in situ production it is useful to define absolute excesses

$$E_M^{(84)} = \left[\left(\frac{Kr^M}{Kr^{84}}\right)_{\text{meteorite}} - \left(\frac{Kr^M}{Kr^{84}}\right)_{\text{AVCC}}\right] Kr^{84}_{\text{meteorite}} \quad (9)$$

These epsilon-values are given in Table 14. The absolute Kr^{80} excess is largest in Mezö-Madaras. It is approximately twice as large in our Abee sample as it is in those of Clarke and Thode [8]. If the $Br^{79}(n,\gamma\beta)Kr^{80}$ reaction is responsible for this Kr^{80} anomaly then the same neutrons should also produce other isotopes, e. g. $Br^{81}(n,\gamma\beta)Kr^{82}$, $I^{127}(n,\gamma\beta)Xe^{128}$, $Cl^{35}(n,\gamma\beta)Ar^{36}$. The presence or absence of an excess in these isotopes will be a crucial test for the neutron capture hypothesis and also for a possible in situ production.

meteorite	$E_M^{(84)} \times 10^{-12}$ cc STP/gm 78	80	82	83	86	$E_{128} \times 10^{-12}$ cc STP/gm
Abee 3	—	14 ± 2	6 ± 3	0 ± 3	-1 ± 4	—
Abee 4	—	12 ± 2	6 ± 3	1 ± 3	-2 ± 3	—
Abee	—	21 ± 2	10 ± 5	-2 ± 4	-3 ± 5	2.5 ± 1
Mezö-Madaras	—	40 ± 4	18 ± 11	-7 ± 10	-6 ± 10	7.5 ± 4

Table 14. Krypton and Xe^{128} excess concentrations in the Abee and Mezö-Madaras meteorites. Abee 3 and 4 data from Clarke and Thode [8]. Abee and Mezö-Madaras this paper. Krypton excesses $E_M^{(84)}$ calculated from Table 12 according to Eq. (9), Xe^{128} excesses E_{128} from Table 11. Concentration errors are not included because they are systematic.

Table 14 shows Kr^{82} excesses outside of the experimental errors for Mezö-Madaras and for all Abee samples. These Mezö-Madaras and Abee samples show also a Xe^{128} excess, as can be seen from Tables 12 and 14. The Ar^{36}/Ar^{38} ratio in Mezö-Madaras[13] does not show an Ar^{36} anomaly due to $Cl^{35}(n,\gamma\beta)Ar^{36}$, and only an upper limit can be given for neutron produced Ar^{36}.

In order to estimate possible relative production rates for different isotopes by (n,γ) processes, we shall calculate the production in three different energy regions: 1) E_{th} to ~ 10 eV (σ_a roughly $\sim 1/v$); 2) $30 - 300$ eV (σ_a determined by several large resonances); and 3) 10 keV – 100 keV (σ_a roughly $\sim 1/E$). The three energy regions sufficiently cover the possible neutron spectra, namely 1) highly moderated, 2) moderated, 3) poorly moderated.

In the first region it is assumed that $\sigma_a \sim 1/v$ for all isotopes, in fairly good agreement with experimental data. The resonance integral R is then

$$R = \int_{E_{th}}^{\infty} \sigma_a \frac{dE}{E} = 2\,\sigma_{th}\,. \tag{10}$$

In the second region, resonance integrals

$$R = g \frac{\hbar^2}{4\,m_N} \frac{\Gamma_n \Gamma_\gamma}{E_0^2\,\Gamma} \tag{11}$$

have to be determined for each resonance in the region and added. The statistical factor g is taken as 1/2. E_0, the resonance energy, and Γ_n, Γ_γ and Γ, the neutron, gamma and total widths respectively are taken from BNL 325 [58] for Br^{79}, Br^{81} and I^{127}. For Cl^{35} R is calculated from measurements of KASHUKEEV, POPOV, and SHAPIRO [59]. The values for Se^{82} and Te^{130} are based on TRURAN's [60] calculations. TRURAN has also obtained cross sections for Br^{79}, Br^{81}, and Cl^{35} which are in satisfactory agreement with the values of BNL 325 [58] and KASHUKEEV et al. [59]. In the third energy region R is based on measured $\sigma(n,\gamma)$ cross sections [58, 59] and on TRURAN's [60] theoretical calculations.

target	$R = 2\,\sigma_{th}$ (E_{th} − 10 eV) barn	R (30−300 eV) barn	R (10−100 keV) barn
Cl^{35}	89 [a]	0.6 [b,c]	0.04 [b,c]
Br^{79}	23 [a]	110 [a]	1.3 [a,c]
Br^{81}	6.6 [a]	42 [a]	0.8 [a,c]
Se^{82}	0.11 [a]	1 [c]	0.04 [c]
I^{127}	11 [a]	130 [a]	2 [a]
Te^{130}	0.46 [a]	1.2 [c]	0.05 [c]

Table 15. Resonance integrals $R = \int \sigma_a (dE/E)$ in three neutron energy intervals for some relevant isotopes. Data from: [a] BNL 325 [58]; [b] KASHUKEEV, POPOV, and SHAPIRO [59]; [c] TRURAN [60].

Table 15 gives the resonance integrals for some relevant nuclei. In Table 16 the concentrations, which should result from (n,γ) reactions in Abee and Mezö-Madaras, are calculated in the three neutron energy regions. The theoretical concentrations are normalized to the observed Kr^{80} excesses. Also given are the integrated neutron slowing down densities required to produce the observed Kr^{80} excesses. They are calculated from

$$N = R \cdot Q/(\xi\,\Sigma_{tot}) \tag{12}$$

assuming constant slowing down density within the energy region in question. N is the number of atoms/cm³ produced per target atom and $\xi\,\Sigma_{tot}$ is 3.54×10^{-2} cm^{-1} for ordinary chondritic material [61].

neutron produced isotope	excess observed 10^{-12} cc STP/gm	theoretical (n,γ) production 10^{-12} cc STP/gm		
		E_{th}−10 eV	30−300 eV	10−100 keV
Abee				
Kr^{80}	21	21	21	21
Kr^{82}	10	6	8	13
Xe^{128}	2.5	0.5	1.3	1.7
Ar^{36}	—	4.2×10^4	60	340
Kr^{83}	<2	0.08	0.15	0.5
Xe^{131}	<12	0.12	0.06	0.2
required Q neutrons/cm³		6.6×10^{13}	1.4×10^{13}	1.2×10^{15}
MezöMadaras				
Kr^{80}	40	40	40	40
Kr^{82}	18	11	15	25
Xe^{128}	7.5	2	5	7
Ar^{36}	$<3 \times 10^4$	1.5×10^5	200	1200
Kr^{83}	<3	0.8	1.5	5
Xe^{131}	<40	0.4	0.25	0.8
required Q neutrons/cm³		1.1×10^{15}	2.3×10^{14}	1.9×10^{16}

Table 16. Comparison of observed excess isotopic abundances with calculated (n,γ) production. The latter have been normalized to the observed Kr^{80} excess. Also given are the integrated neutron slowing down densities Q required to produce the observed Kr^{80} excess in each interval. Average hypersthene chondrite chemical composition has been assumed for Mezö-Madaras.

Thermal or slow neutrons ($E < 10$ eV) cannot account for the observed Kr^{80} excess for two reasons: a) the predicted Ar^{36} excess is not observed in Mezö-Madaras; b) a situation where the slowing down density is much higher at E_{th} to 10 eV than it is at 30 to 300 eV is very unlikely in nature. Thus, intermediate or fast neutrons must be responsible for the Kr^{80} anomaly, and quite possibly a considerable fraction is produced by the resonances in the 30 to 300 eV region. The production ratio

[58] Neutron Cross Sections, compiled by D. J. HUGHES and R. B. SCHWARTZ, BNL 325 second edition [1958] and Supplement No. 1 [1960].

[59] N. T. KASHUKEEV, YU. P. POPOV, and E. L. SHAPIRO, J. Nucl. Energy, parts A and B, **14**, 76 [1961].

[60] J. W. TRURAN, unpublished calculations based on the method given by J. W. TRURAN, C. J. HANSEN, A. G. W. CAMERON, and A. GILBERT, Thermonuclear Reaction Rates in Medium and Heavy Nuclei (preprint 1965).

[61] P. EBERHARDT, J. GEISS, and H. LUTZ, in Earth Science and Meteoritics, dedicated to F. G. HOUTERMANS (J. GEISS and E. D. GOLDBERG ed.), North Holland Publ. Co., Amsterdam 1963, p. 143.

Kr^{80}/Kr^{82} would then be approximately 2.5, in excellent agreement with the observed $(Kr^{80}/Kr^{82})_{excess}$ ratios (cf. Table 14). Also the calculated $(Xe^{128}/Kr^{80})_{excess}$ ratios are in satisfactory agreement with the observed Xe^{128} excesses. Therefore, no doubt remains that the Kr^{80}, Kr^{82} and Xe^{128} excesses given in Table 14 are indeed due to (n,γ) reactions of medium energy or fast neutrons.

9.1 Sources of Neutrons

During the exposure of the meteorite to the cosmic radiation, secondary neutrons are produced in the nuclear interactions. These neutrons are then moderated inside the meteorite. EBERHARDT, GEISS, and LUTZ [61] have extensively treated this problem and calculated slowing down densities of comic ray produced neutrons in stone meteorites. In small meteorites virtually all the neutrons escape and therefore slowing down densities are strongly size dependent.

In order to obtain the Q-values given in Table 16 during the radiation age of the meteorites slowing down densities of $q' = 0.07$ neutrons cm^{-3} sec^{-1} for Abee and $q' = 0.28$ neutrons cm^{-3} sec^{-1} for Mezö-Madaras would be required in the energy range of 30 eV to 300 eV. Such slowing down densities only occur in meteorites (spherical shape) with radii larger than 30 cm and 55 cm respectively. These limits may be $10-20\%$ too high, because we have neglected the relatively small production outside of the $30-300$ eV energy interval. These radii would correspond to minimal pre-atmospheric weights of 220 kg for Abee and of 1.4 tons for Mezö-Madaras. The required mass for Abee seems not unreasonable, the recovered weight being 107 kg. From upper limits for neutron induced Cl^{36} activity in the same Abee sample BEGEMANN and VILCSEK [62] have derived an upper limit of 27 cm for the pre-atmospheric radius of Abee.

The recovered weight of Mezö-Madaras is only 23 kg. However, this meteorite fall is described by KNÖPFLER [63, 9] as follows: "After the appearance of a luminous meteor and detonations, a shower of many stones fell, of which the largest weighed about 10 kg". Thus, it may well be that Mezö-Madaras was a larger meteorite and that the main mass of the fall was never recovered. The observed Ne^{22}/Ne^{21} ratio would also be in agreement with a larger mass [13]. Mezö-Madaras is a relatively unaltered (primitive) meteorite [64] and its bromine and iodine content could be higher than the assumed average hypersthene chondrite values. Also the hydrogen content might be above average and thus the neutron moderation more effective. Both effects would considerably lower the required minimal mass.

For the Kr^{80} (n,γ) excesses in Bruderheim and H-Ausson, only upper limits of 1×10^{-12} cc STP/gm can be given. This seems somewhat astonishing because Bruderheim is a large meteorite. However, the Bruderheim sample of CLARKE and THODE [6] has a Xe^{128} excess of 8×10^{-12} cc STP/gm. The Kr isotopic composition is not known in their sample. It thus seems that our sample has either much lower Br and I contents or that it was located close to the pre-atmospheric surface of the meteorite.

There remains little doubt that the observed Kr^{80}, Kr^{82}, and Xe^{128} excesses in Abee are indeed due to cosmic ray produced neutrons. The same explanation for Mezö-Madaras would require that the meteorite was either much larger than indicated by the recovered mass or that it has above average H, Br, and I contents. Some evidence in favor for both requirements exists. At the present time it seems not necessary to invoke any "early irradiation" (neutral or charged) in order to explain the observed Kr^{80}, Kr^{82}, and I^{128} excesses.

Acknowledgements

We are very grateful to Prof. W. SCHOLLER, Vienna; Prof. R. E. FOLINSBEE, Edmonton and Dr. F. BEGEMANN, Mainz for providing us with meteorite samples. To Drs. H. DULAKAS and A. WYTTENBACH we are indebted for their unpublished results of Ca, Fe, Sr, and Ba determinations, to Dr. G. REED for unpublished Br and I concentrations, and to Dr. J. TRURAN for his unpublished cross section calculations. We would like to thank Drs. A. G. W. CAMERON, N. GRÖGLER, and F. G. HOUTERMANS for many stimulating discussions.

This work was supported by the Swiss National Science Foundation, Grants NF 2648, NF 3045, and NF 3468.

[62] F. BEGEMANN and E. VILCSEK, Z. Naturforschg. **20 a**, 533 [1965].

[63] W. KNÖPFLER, Verh. Siebenbürg. Ver. Naturwiss., Hermannstadt **4**, 19 [1853].

[64] J. A. WOOD, private communication 1964.